Organic Electronics 10 (2009) 871–876

Contents lists available at ScienceDirect

Organic Electronics

journal homepage: www.elsevier.com/locate/orgel

Efficient red electrophosphorescence from a fluorene-based bipolar host material

Chen-Han Chien [a,b], Fang-Ming Hsu [a,b], Ching-Fong Shu [a,*], Yun Chi [b,*]

[a] Department of Applied Chemistry, National Chiao Tung University, 300 Hsinchu, Taiwan
[b] Department of Chemistry, National Tsing Hua University, 300 Hsinchu, Taiwan

ARTICLE INFO

Article history:
Received 25 February 2009
Received in revised form 1 April 2009
Accepted 23 April 2009
Available online 5 May 2009

PACS:
71.20.Rv
72.80.Le
73.61.Ph
78.60.Fi

Keywords:
OLED
Electrophosphorescence
Bipolar host material
Red-emitting
White-emitting

ABSTRACT

We have prepared efficient red organic light-emitting diodes (OLEDs) incorporating 2,7-bis(diphenylphosphoryl)-9-[4-(*N*,*N*-diphenylamino)phenyl]-9-phenylfluorene (POAPF) as the host material doped with the osmium phosphor $Os(fptz)_2(PPh_2Me)_2$ (fptz = 3-trifluoromethyl-5-pyridyl-1,2,4-triazole). POAPF, which possesses bipolar functionalities, can facilitate both hole- and electron-injection from the charge transport layers to provide a balanced charge flux within the emission layer. The peak electroluminescence performance of the device reached as high as 19.9% and 34.5 lm/W – the highest values reported to date for a red phosphorescent OLED. In addition, we fabricated a POAPF-based white light OLED – containing red-[doped with $Os(fptz)_2(PPh_2Me)_2$] and blue-emitting {doped with iridium(III) bis[(4,6-difluorophenyl)pyridinato-*N*,$C^{2'}$] picolinate, FIrpic} layers – that also exhibited satisfactory efficiencies (18.4% and 43.9 lm/W).

© 2009 Elsevier B.V. All rights reserved.

1. Introduction

Phosphorescent organic light-emitting diodes (OLEDs) attract a great deal of attention because they can theoretically approach 100% internal quantum efficiency by harnessing both singlet and triplet excitons [1–6]. In these phosphorescent devices, the organometallic phosphors are commonly doped into appropriate host materials to prevent concentration quenching and achieve high efficiency [1,2]. The past few years have witnessed the development of blue and green phosphorescent OLEDs exhibiting high external quantum efficiencies (EQEs) and power efficiencies (PEs) [4,7–12]. There are, however, far fewer reports describing high-performance red phosphorescent OLEDs. Being one of the primary colors, red emission from OLEDs is important for applications in full-color displays and solid state lighting [13–19]. For future device applications, it will be essential for OLEDs to exhibit efficient, saturated red emissions.

Since Baldo et al. developed the concept of phosphorescent OLEDs [1], the carbazole derivative 4,4′-*N*,*N*′-dicarbazolebiphenyl (CBP) has been used widely as a host material for red phosphorescent OLEDs [3,20–27] because of its suitable triplet energy (E_T) and good hole-transporting ability. Because CBP has a wide band gap (E_g), injecting carriers are often required to overcome the large energy barriers between the charge transport layers and its highest occupied molecular orbital (HOMO) and/or lowest unoccupied molecular orbital (LUMO). In addition, the poor match

* Corresponding authors. Tel.: +886 3 5712121x56544; fax: +886 3 5723764 (C.-F. Shu).
E-mail address: shu@cc.nctu.edu.tw (C.-F. Shu).

1566-1199/$ - see front matter © 2009 Elsevier B.V. All rights reserved.
doi:10.1016/j.orgel.2009.04.013

between the energy levels of CBP and the red triplet dopants usually results in direct charge trapping within the emitting layer (EML). Therefore, red phosphorescent devices based on CBP often require high operation voltages and provide unsatisfactory PEs. To break free from these constraints, several attempts have been made recently to use host materials possessing narrower band gaps [28–30] or bipolar characteristics [31–33] to improve the charge injection and electroluminescence (EL) performance of red phosphorescent OLEDs. Nevertheless, the PEs of the red electrophosphorescence remain far below those reported for blue- or green-emitting devices [3,20–27].

In this paper, we report the fabrication of efficient red phosphorescent OLEDs incorporating the bipolar host 2,7-bis(diphenylphosphoryl)-9-[4-(*N*,*N*-diphenylamino) phenyl]-9-phenylfluorene (POAPF) doped with the efficient red-emitting phosphor $Os(fptz)_2(PPh_2Me)_2$ (fptz = 3-trifluoromethyl-5-pyridyl-1,2,4-triazole); Fig. 1 presents their chemical structures. This charge–neutral osmium complex has been used previously as a phosphor in red-emitting devices displaying high EQEs [22,34]. The relatively low oxidation potential of $Os(fptz)_2(PPh_2Me)_2$, however, results in severe charge trapping in devices using CBP as the host, resulting in high driving voltages and unsatisfactory PEs. POAPF, which contains an electron-rich triphenylamine group and an electron-deficient bis(diphenylphosphoryl)fluorene unit [35–37], has recently been developed as a host material exhibiting bipolar characteristics [38] that not only provide suitable frontier orbital energies for facile hole- and electron-injection but also improve the balance of charge flux in the emission layer. Moreover, the triplet energy (E_T) of POAPF is estimated to be 2.72 eV – a value that is sufficiently high for POAPF to act as a host material for red, green, and even blue phosphorescent emitters. Indeed, blue phosphorescent OLEDs based on POAPF doped with FIrpic can exhibit high values of EQE and PE [38]. We expected that POAPF could also be utilized as a host for the red-emitting $Os(fptz)_2(PPh_2Me)_2$, thereby improving charge injection and enhancing charge balance to result in highly efficient red phosphorescent devices.

2. Experimental

The bipolar host molecule POAPF [38] and the red phosphorescent emitter $Os(fptz)_2(PPh_2Me)_2$ [22] were prepared using previously reported procedures. The hole-transport material 4,4′-bis(3-methylphenylphenylamino)biphenyl (TPD), the conventional host material CBP, and the electron-transport material 4,7-diphenyl-1,10-phenanthroline (BPhen) were all purchased from LumTec Corp. and used without further purification.

The oxidation and reduction potentials were measured, respectively, in anhydrous CH_2Cl_2 and anhydrous DMF, containing 0.1 M $TBAPF_6$ as the supporting electrolyte, at a scan rate of 50 mV/s against a Ag/Ag^+ (0.01 M $AgNO_3$) reference electrode, with ferrocene as the internal standard. The onset potentials were determined from the intersection of two tangents drawn at the rising current and background current of the cyclic voltammogram.

The EL devices were fabricated through vacuum deposition (10^{-6} torr) of the materials onto ITO glass (sheet resistance: 25 Ω/square). All of the organic layers were deposited at a rate of 1.0 Å/s. The cathode was completed through thermal deposition of LiF (15 Å; deposition rate: 0.1 Å/s) and then capping with Al metal (100 nm) through thermal evaporation (deposition rate: 4.0 Å/s). The current–voltage–luminance relationships of the devices were measured using a Keithley 2400 source meter and a Newport 1835C optical meter equipped with an 818ST silicon photodiode. The EL spectrum was obtained using a Hitachi F4500 spectrofluorimeter.

3. Results and discussion

Fig. 2 presents the current density–voltage (*I*–*V*) characteristics of the hole-only devices having the configuration indium tin oxide (ITO)/TPD (30 nm)/host material (30 nm)/TPD (30 nm)/Al (100 nm) and the electron-only devices having the configuration ITO/BPhen (30 nm)/host material (30 nm)/BPhen (30 nm)/LiF (15 Å)/Al (100 nm). Here, "host material" refers to either the bipolar host POAPF or the conventional host CBP. Because of the high LUMO energy level (−2.20 eV) of TPD in the hole-only devices and the low HOMO energy level (−6.40 eV) of BPhen in the electron-only devices, injections of electrons and holes were prohibited in the hole- and electron-only devices, respectively; accordingly, the measured *I*–*V* characteristics were dominated by holes and electrons, respectively. Fig. 2 reveals that the POAPF-based devices exhibited lower turn-on voltages and higher current densities than did the CBP-based devices under the same bias.

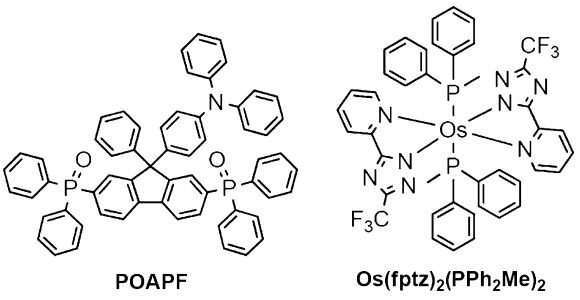

Fig. 1. Chemical structures of POAPF and $Os(fptz)_2(PPh_2Me)_2$.

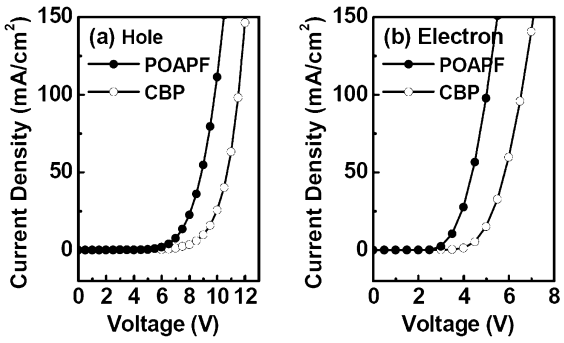

Fig. 2. Current density–voltage (*I*–*V*) curves of (a) hole- and (b) electron-only devices.

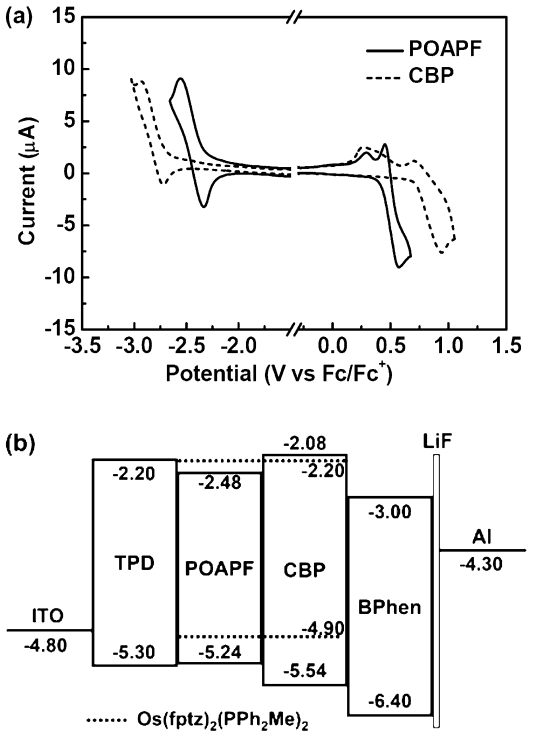

Fig. 3. (a) Cyclic voltammograms of POAPF and CBP, recorded at a scan rate of 50 mV/s. (b) Energy level diagram of the red phosphorescent devices.

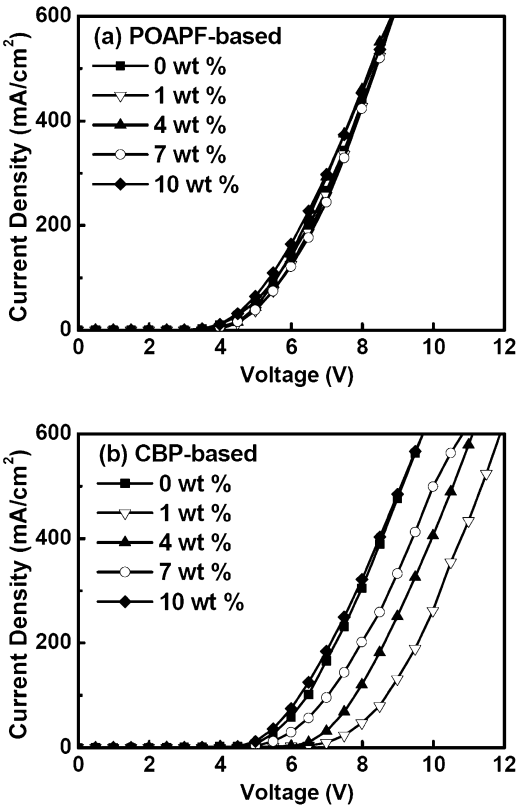

Fig. 4. *I–V* characteristics of devices incorporating (a) POAPF and (b) CBP as hosts at various doping concentrations.

The reduced driving voltages in the POAPF-based devices may be due to the decrease in barrier heights for hole- and electron-injection from the charge transport layers (CTLs) to POAPF.

To further understand the improved injection of holes and electrons in the POAPF-based devices, we employed cyclic voltammetry (CV) to estimate the HOMO and LUMO energy levels of POAPF and CBP (Fig. 3a), using a three-electrode cell with ferrocene as the internal standard. Because of its triphenylamine donor unit, POAPF exhibits a lower onset of its oxidation potential (0.44 V) relative to that of CBP (0.74 V). On the other hand, the onset of the reduction potential of POAPF (−2.32 V), originating from its bis(diphenylphosphoryl)fluorene unit, is significantly less negative than that of CBP (−2.72 V). On the basis of these onset values for oxidation and reduction, we estimated the HOMO and LUMO energy levels of POAPF (−5.24 and −2.48 eV, respectively) and CBP (−5.54 and −2.08 eV, respectively) relative to ferrocene (4.80 eV below the vacuum) as a reference [39]. According to the energy level diagram in Fig. 3b, the hole-injection barrier from TPD and the electron-injection barrier from BPhen to the POAPF layer were both considerably lower than those to the CBP layer. As a result, the presence of POAPF facilitates hole- and electron-injection, as observed in the hole- and electron-only measurements (*vide supra*).

Using POAPF as the host material, we fabricated red OLEDs in the configuration ITO/TPD (30 nm)/R-EML (30 nm)/BPhen (30 nm)/LiF (15 Å)/Al (100 nm), where TPD and BPhen were employed as hole- and electron-transporting layers, respectively, and R-EML refers to the POAPF layer doped with various concentrations of $Os(fptz)_2(PPh_2Me)_2$. For comparison, we also fabricated reference devices incorporating CBP as the host. Fig. 4 depicts the *I–V* characteristics of these red-emitting OLEDs. As expected, the POAPF-based devices exhibited significantly higher current densities than did the CBP-based devices under the same bias. The *I–V* characteristics of the POAPF-based devices underwent no apparent changes when we increased the doping concentration of $Os(fptz)_2(PPh_2Me)_2$ from 0 to 10 wt%. This phenomenon can be explained by considering the energy level diagram of the devices (Fig. 3b). Because the HOMO energy level of $Os(fptz)_2(PPh_2Me)_2$ is merely 0.34 eV higher than that of POAPF, it behaves as a less-effective trapping sites for holes; meanwhile, because the LUMO energy level of $Os(fptz)_2(PPh_2Me)_2$ is 0.28 eV above that of POAPF, electrons injected from the BPhen layer into the POAPF layer are mostly transported through the POAPF layer without being trapped in the osmium phosphor. Thus, varying the concentration of $Os(fptz)_2(PPh_2Me)_2$ in the EML should not significantly alter the degree of charge injection in POAPF-based devices. On the other hand, the current density of the CBP-based devices exhibited a strong dependence on the doping concentration. Because the HOMO energy level of $Os(fptz)_2(PPh_2Me)_2$ is 0.64 eV higher than that of CBP, holes can potentially be trapped at

Table 1
Device performance.

Device	Red		White
Host	POAPF	CBP	POAPF
Turn-on voltage [V][a]	2.3	3.5	2.2
Max. EQE [%]	19.9	13.2	18.4
Max. LE [cd/A]	32.8	21.4	34.5
Max. PE [lm/W]	34.5	13.4	43.9
Voltage [V][b]	3.7	5.1	3.0
EQE [%][b]	18.6	13.1	14.9
LE [cd/A][b]	30.6	21.1	27.9
PE [lm/W][b]	26.1	13.1	29.5
EL λ_{max} [nm][c]	616	616	472, 498, 612
CIE, x and y[c]	(0.64, 0.36)	(0.64, 0.36)	(0.38, 0.34)

[a] Recorded at 1 cd/m^2.
[b] Recorded at 1000 cd/m^2.
[c] At 5 V.

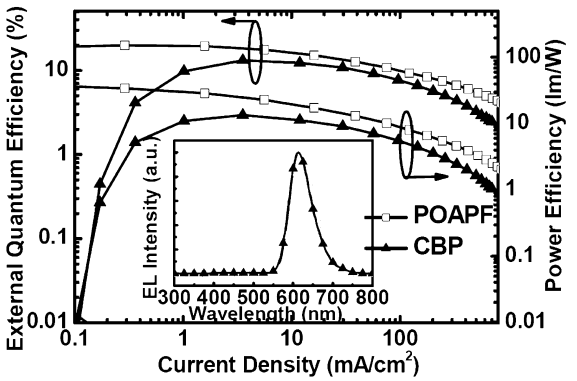

Fig. 5. EQE and PE of 7 wt% Os(fptz)$_2$(PPh$_2$Me)$_2$-doped POAPF- and CBP-based devices plotted with respect to the current density. Inset: EL spectra (applied voltage: 5 V) of the POAPF- and CBP-based devices.

Os(fptz)$_2$(PPh$_2$Me)$_2$ at low doping concentrations. When the concentration of the osmium phosphor was increased, we attribute the resulting increased hole-injection efficiency to direct charge injection from the hole-transporting layer (HTL) into Os(fptz)$_2$(PPh$_2$Me)$_2$. Accordingly, employing POAPF as the host for Os(fptz)$_2$(PPh$_2$Me)$_2$ significantly reduced the degree of charge trapping within the EML.

The optimal performances of both the POAPF- and CBP-based devices occurred at a doping concentration of 7 wt%. Table 1 lists the key characteristics of these red electrophosphorescent devices. The POAPF-based red-emitting device had a relatively low turn-on voltage of 2.3 V (corresponding to 1 cd/m^2) and, at a practical brightness of 1000 cd/m^2, its driving voltage was merely 3.7 V. These values are much lower than those of the CBP-based device (3.5 and 5.1 V, respectively). We ascribe the reduced driving voltage of the POAPF-based device to facile hole/electron-injections and less-effective charge trapping within this bipolar host. Fig. 5 presents the EQE and PE profiles plotted with respect to the current density. The POAPF-based device exhibited a maximum EQE of 19.9% (at a luminance of 96 cd/m^2) – 1.5 times greater than that of its CBP-based counterpart (13.2%). These values reveal that the presence of the bipolar host material resulted in balanced charge fluxes within the EML and, therefore, a high EQE. Notably, the PE of the POAPF-based device (34.5 lm/W) was 2.5 times higher than that of its CBP-based counterpart (13.4 lm/W). We attribute this large enhancement in device performance to the substantially lower driving voltage and improved charge balance within the POAPF-based device. In addition to its highly efficient device performance, the POAPF-based OLED displayed a less-problematic efficiency roll-off at higher luminance. The efficiencies remained fairly high (18.6% and 26.1 lm/W) at a practical luminance of 1000 cd/m^2. Our POAPF-based red-emitting device possesses superior EL performance, particularly in terms of its PE (Table 2), relative to those of previously reported red electrophosphorescent OLEDs [29,31,32,34]. Both the POAPF- and CBP-based devices emitted saturated red light (each main peak at 616 nm) and Commission Internationale de L'Eclairage (CIE) coordinates of (0.64, 0.36) at 5 V (inset to Fig. 5).

To further utilize the superior host properties of POAPF, we fabricated white light-emitting devices – featuring red emission from Os(fptz)$_2$(PPh$_2$Me)$_2$ and complementary blue/green emission from FIrpic – having the configuration ITO/TPD (30 nm)/R-EML (x nm)/B-EML (30−x nm)/BPhen (30 nm)/LiF (15 Å)/Al (100 nm). Here, we used POAPF as the bipolar host material for both the red EML [R-EML; doped with 7 wt% Os(fptz)$_2$(PPh$_2$Me)$_2$] and the blue EML (B-EML; doped with 7 wt% FIrpic); the total thickness of these dual emission layers was fixed at 30 nm in each device. To realize white light emission from such composite emission systems, we adjusted the thickness ratio at various compositions to achieve appropriate fractions of excitons for both triplet emitters. Fig. 6 reveals an increase in the blue emission intensity relative to red emission upon decreasing the thickness of the R-EML. We obtained white emission when the thicknesses of the R-EML and B-EML were 1 and 29 nm, respectively. This white-emitting device also exhibited a low turn-on voltage (2.2 V) and an applicable luminance of 1000 cd/m^2 at merely 3.0 V (Fig. 7a); its maximum EQE reached 18.4% at a luminance of 90 cd/m^2. As a result of the low driving voltage, the PE reached as high as 43.9 lm/W (Fig. 7b). Even when the luminance

Table 2
Performance of red electrophosphorescent devices.

Host	Dopant	Max. EQE [%]	Max. PE [lm/W]	CIE (x, y)	Ref.
POAPF	Os(fptz)$_2$(PPh$_2$Me)$_2$	19.9	34.5	(0.64, 0.36)	This study
(ppy)$_2$Ir(acac)	Ir(piq)$_3$	9.2	11.0	(0.65, 0.35)	[29]
D2ACN	Mpq$_2$Iracac	10.8	13.0	(0.66, 0.34)	[31]
o-CzOXD	Ir(piq)$_2$acac	18.5	11.5	(0.68, 0.32)	[32]
TFTPA	Os(fptz)$_2$(PPh$_2$Me)$_2$	18.0	25.2	(0.64, 0.36)	[34]

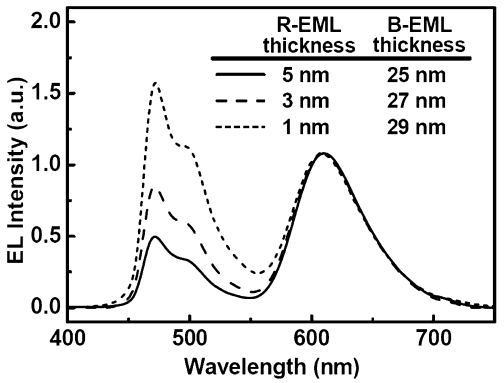

Fig. 6. EL spectra of dual-emission devices (applied voltage: 5 V) incorporating various thicknesses of their R-EML and B-EML.

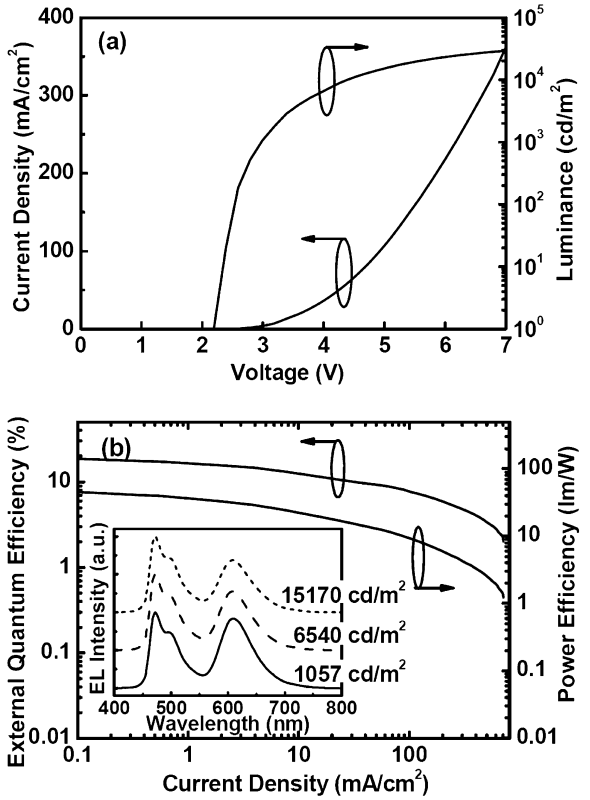

Fig. 7. Plots of (a) current density and luminance with respect to the voltage and (b) EQE and PE with respect to the current density for the white light-emitting device. Inset: EL spectra recorded at various luminances.

was 1000 cd/m^2, the EL efficiencies remained high (14.9% and 29.5 lm/W). The EL efficiency of this white electrophosphorescence is among the highest values ever reported for white light-emitting diodes [12,40,41]. The EL spectra of this device revealed a virtually stable white color emission (inset to Fig. 7b). The CIE coordinates shifted slightly from (0.40, 0.34) at a luminance of 1057 cd/m^2 to (0.38, 0.34) at 15,170 cd/m^2; nevertheless, the color coordinates remained in the white light region.

4. Conclusion

We have realized highly efficient red electrophosphorescence in OLEDs incorporating the bipolar host POAPF doped with the red-emitting osmium phosphor $Os(fptz)_2(PPh_2Me)_2$. The bipolar characteristics of POAPF resulted in the red-emitting devices exhibiting very low driving voltages and achieving EL efficiencies as high as 19.9% and 34.5 lm/W – the highest performance of any red phosphorescent OLED reported to date – with a saturated red emission located at CIE coordinates of (0.64, 0.36). In addition, we used POAPF to fabricate a white light-emitting device possessing a dual EML configuration; it also exhibited satisfying efficiencies (18.4% and 43.9 lm/W). The white emission remained stable, with the CIE coordinates shifting slightly from (0.40, 0.34) at a luminance of 1057 cd/m^2 to (0.38, 0.34) at 15,170 cd/m^2. The performance of these phosphorescent devices makes them very attractive materials for potential commercial applications.

Acknowledgment

We thank the National Science Council for financial support.

References

[1] M.A. Baldo, D.F. O'Brien, Y. You, A. Shoustikov, S. Sibley, M.E. Thompson, S.R. Forrest, Nature 395 (1998) 151.
[2] M.A. Baldo, S. Lamansky, P.E. Burrows, M.E. Thompson, S.R. Forrest, Appl. Phys. Lett. 75 (1999) 4.
[3] S. Lamansky, P. Djurovich, D. Murphy, F. Abdel-Razzaq, H.E. Lee, C. Adachi, P.E. Burrows, S.R. Forrest, M.E. Thompson, J. Am. Chem. Soc. 123 (2001) 4304.
[4] C. Adachi, M.A. Baldo, M.E. Thompson, S.R. Forrest, J. Appl. Phys. 90 (2001) 5048.
[5] E.L. Williams, K. Haavisto, J. Li, G.E. Jabbour, Adv. Mater. 19 (2007) 197.
[6] S. Watanabe, N. Ide, J. Kido, Jpn. J. Appl. Phys. 46 (2007) 1186.
[7] M. Ikai, S. Tokito, Y. Sakamoto, T. Suzuki, Y. Taga, Appl. Phys. Lett. 79 (2001) 156.
[8] S.J. Yeh, M.F. Wu, C.T. Chen, Y.H. Song, Y. Chi, M.H. Ho, S.F. Hsu, C.H. Chen, Adv. Mater. 17 (2005) 285.
[9] M.H. Tasi, H.W. Lin, H.C. Su, T.H. Ke, C.C. Wu, F.C. Fang, Y.L. Liao, K.T. Wong, C.I. Wu, Adv. Mater. 18 (2006) 1216.
[10] D. Tanaka, H. Sasabe, Y.J. Li, S.J. Su, T. Takeda, J. Kido, Jpn. J. Appl. Phys. 46 (2007) L10.
[11] S.J. Su, T. Chiba, T. Takeda, J. Kido, Adv. Mater. 20 (2008) 2125.
[12] S.J. Su, E. Gonmori, H. Sasabe, J. Kido, Adv. Mater. 20 (2008) 4189.
[13] C.W. Tang, S.A. VanSlyke, Appl. Phys. Lett. 51 (1987) 913.
[14] C.W. Tang, S.A. VanSlyke, C.H. Chen, J. Appl. Phys. 65 (1989) 3610.
[15] M.A. Baldo, M.E. Thompson, S.R. Forrest, Nature 403 (2000) 750.
[16] T. Fuhrmann, J. Salbeck, MRS Bull. 28 (2003) 354.
[17] B.W. D'Andrade, R.J. Holmes, S.R. Forrest, Adv. Mater. 16 (2004) 624.
[18] B.W. D'Andrade, S.R. Forrest, Adv. Mater. 16 (2004) 1585.
[19] H. Kanno, R.J. Holmes, Y. Sun, S. Kena-Cohen, S.R. Forrest, Adv. Mater. 18 (2006) 339.
[20] A. Tsuboyama, H. Iwawaki, M. Furugori, T. Mukaide, J. Kamatani, S. Igawa, T. Moriyama, S. Miura, T. Takiguchi, S. Okada, M. Hoshino, K. Ueno, J. Am. Chem. Soc. 125 (2003) 12971.
[21] C.H. Yang, C.C. Tai, I.W. Sun, J. Mater. Chem. 14 (2004) 947.
[22] Y.L. Tung, S.W. Lee, Y. Chi, Y.T. Tao, C.H. Chien, Y.M. Cheng, P.T. Chou, S.M. Peng, C.S. Liu, J. Mater. Chem. 15 (2005) 460.
[23] C.L. Li, Y.J. Su, Y.T. Tao, P.T. Chou, C.H. Chien, C.C. Cheng, R.S. Liu, Adv. Funct. Mater. 15 (2005) 387.
[24] D.K. Rayabarapu, B.M.J.S. Paulose, J.P. Duan, C.H. Cheng, Adv. Mater. 17 (2005) 349.
[25] Y.L. Tung, S.W. Lee, Y. Chi, L.S. Chen, C.F. Shu, F.I. Wu, A.J. Carty, P.T. Chou, S.M. Peng, G.H. Lee, Adv. Mater. 17 (2005) 1059.
[26] S. Takizawa, Y. Sasaki, M. Akhtaruzzaman, H. Echizen, J. Nishida, T. Iwata, S. Tokito, Y. Yamashita, J. Mater. Chem. 17 (2007) 841.

[27] C.L. Ho, W.Y. Wong, Z.Q. Gao, C.H. Chen, K.W. Cheah, B. Yao, Z. Xie, Q. Wang, D. Ma, L. Wang, X.M. Yu, H.S. Kwok, Z. Lin, Adv. Funct. Mater. 18 (2008) 319.
[28] T. Tsuzuki, Y. Nakayama, J. Nakamura, T. Iwata, S. Tokito, Appl. Phys. Lett. 88 (2006) 243511.
[29] T. Tsuzuki, S. Tokito, Adv. Mater. 19 (2007) 276.
[30] T.J. Park, W.S. Jeon, J.J. Park, S.Y. Kim, Y.K. Lee, J. Jang, J.H. Kwon, R. Pode, Appl. Phys. Lett. 92 (2008) 113308.
[31] W.Y. Hung, T.C. Tsai, S.Y. Ku, L.C. Chi, K.T. Wong, Phys. Chem. Chem. Phys. 10 (2008) 5822.
[32] Y. Tao, Q. Wang, C. Yang, Q. Wang, Z. Zhang, T. Zou, J. Qin, D. Ma, Angew. Chem. Int. Ed. 47 (2008) 8104.
[33] Y. Tao, Q. Wang, Y. Shang, C. Yang, L. Ao, J. Qin, D. Ma, Z. Shuai, Chem. Commun. (2009) 77.
[34] C.H. Wu, P.I. Shih, C.F. Shu, Y. Chi, Appl. Phys. Lett. 92 (2008) 233303.
[35] A.B. Padmaperuma, L.S. Sapochak, P.E. Burrows, Chem. Mater. 18 (2006) 2389.
[36] S.O. Jeon, K.S. Yook, C.W. Joo, J.Y. Lee, Appl. Phys. Lett. 94 (2009) 013301.
[37] F.M. Hsu, C.H. Chien, P.I. Shih, C.F. Shu, Chem. Mater. 21 (2009) 1017.
[38] F.M. Hsu, C.H. Chien, C.-F. Shu, C.H. Lai, C.C. Hsieh, K.W. Wang, P.T. Chou, submitted for publication.
[39] J. Pommerehne, H. Vestweber, W. Guss, R.F. Mahrt, H. Bässler, M. Porsch, J. Daub, Adv. Mater. 7 (1995) 551.
[40] Y. Sun, S.R. Forrest, Appl. Phys. Lett. 91 (2007) 263503.
[41] G. Schwartz, M. Pfeiffer, S. Reineke, K. Walzer, K. Leo, Adv. Mater. 19 (2007) 3672.